

On the Use of Detailed Models in the MPC Algorithm: The Pressure-Swing Distillation Case

Davide Fissore, Marco Pin, and Antonello A. Barresi

Dipartimento di Scienza dei Materiali ed Ingegneria Chimica, Politecnico di Torino, 10129 Torino, Italy

DOI 10.1002/aic.10953

Published online August 8, 2006 in Wiley InterScience (www.interscience.wiley.com).

A novel approach to the design of a model predictive control (MPC) algorithm for a complex plant (with energy integration and mass recycles) is given. Sensitivity analysis and steady-state optimization are used to determine the manipulated variables that have the strongest influence on the objective function of the operation. This allows a reduction of the number of variables that are optimized on-line, as well as the use of detailed, first-principle-based models in the MPC algorithm, thus resulting in more reliable predictions. Moreover, the same algorithm can be used to control plants of different size, without the need of a new calibration of the parameters of the model. The application of this procedure to a pressure-swing distillation unit is given as an example. © 2006 American Institute of Chemical Engineers AIChE J, 52: 3491–3500, 2006

Keywords: process control, model predictive control (MPC), optimization, process modeling, pressure-swing distillation

Introduction

Model predictive control (MPC) is an appropriately descriptive name for a class of control schemes that use a process model for two tasks:

- (1) Explicit prediction of future plant behavior
- (2) Computation of the suitable control actions required to drive the controlled variable to the desired target value, that is, to minimize the offset over a time interval known as the prediction horizon:

$$\min_u \left\{ \sum_{i=1}^{h_p} [y(i) - y_{set}(i)]^2 \right\} \quad (1)$$

In Eq. 1 $y(i)$ is the value of the controlled variable at the time instant i , $y_{set}(i)$ is the set point value for the variable y at the same time instant, and h_p is the *prediction horizon*, that is, the number of time intervals in the future where the evolution of the system is predicted given the initial state and the sequence

of control actions. Obviously an MPC algorithm can handle multivariable problems: in this case y is the array of the controlled variables and y_{set} is the array of their set point values.

Several authors have published excellent reviews about MPC theoretical issues.^{1–7} MPC technology was originally developed to control power plants and petroleum refineries; presently, it has found application in a wide variety of areas, including chemicals, food processing, automotive, aerospace, metallurgy, and pulp and paper processes. It owes its popularity to the possibility of handling nonlinear control problems and of including in the problem definition any kind of constraints because it is posed as an optimization problem. A wide variety of MPC schemes are currently available as commercial software packages; what differentiates one specific scheme from the others is the strategy and philosophy underlying how each element is implemented.

For a generic discrete input/output model such as

$$\hat{y}(k) = g[u(k-1), u(k-2), \dots, u(k-n_a), \hat{y}(k-1), \hat{y}(k-2), \dots, \hat{y}(k-n_b)] \quad (2)$$

where $\hat{y}(k)$ is the prediction of the controlled variables at the time instant k obtained by means of a mathematical model, $u(k)$

Correspondence concerning this article should be addressed to A. A. Barresi at antonello.barresi@polito.it.

represents the values of the manipulated variables at the time instant k , n_a and n_b are the number of time intervals where the input and the output are evaluated, the MPC algorithm evaluates the sequence of manipulated variables that minimizes the function

$$\min_{u(k), \dots, u(k+h_c-1)} \left\{ \sum_{i=k+1}^{k+h_p} \omega_y [\hat{y}(i) - y_{set}(i)]^2 + \sum_{i=k}^{k+h_c-1} \omega_u [u(i) - u(i-1)]^2 \right\} \quad (3)$$

where $y_{set}(i)$ is the set point for the controlled variable y at the time instant i , h_p is the prediction horizon, $u(k), \dots, u(k+h_c-1)$ is the sequence of control actions, and h_c is the control horizon, that is, the number of time intervals in the future where the values of the manipulated variables are calculated. The prediction horizon may be larger than the control horizon; in this case, the manipulated variables maintain, in the time interval between h_c and h_p , the values they have in the final instant of the control horizon.

Even if $h_c > 1$, and thus the result of the minimization is the entire sequence of manipulated variables up to h_c , only the first control action is implemented and the minimization is repeated in the subsequent time interval.

The difference between the set point value of the controlled variable (or variables) and its present value is minimized in the MPC algorithm, as is the difference between two subsequent control actions. These terms are multiplied by two weights, ω_y and ω_u , respectively: if the value of ω_y is increased, then the algorithm will give much more relevance to the offset between the set point and the controlled variables, whereas if ω_u is increased the algorithm will also try to minimize the control effort.

A feedback contribution is needed to take into consideration modeling mismatch with the process.⁸ The modeling mismatch $\delta(k) = y(k) - \hat{y}(k)$ can be evaluated at the time instant k and it can be added to the predictions of the model along the entire prediction horizon, thus leading to the following modified objective function⁹:

$$\min_{u(k), \dots, u(k+h_c-1)} \left\{ \sum_{i=k+1}^{k+h_p} \omega_y \{y_{set}(i) - [\hat{y}(i) + \delta(k)]\}^2 + \sum_{i=k}^{k+h_c-1} \omega_u [u(i) - u(i-1)]^2 \right\} \quad (4)$$

Linear models are generally used to calculate the process evolution in an MPC algorithm. Incorporation of nonlinear dynamics is a relatively recent innovation and most of the issues involving the practical implementation are still unresolved: the most critical one remains that of using appropriate nonlinear models. In fact, it can be difficult to obtain accurate first-principle models when the process is "complex", that is, in the presence of mass recycles and energy integrations. Moreover, the optimization can become too time consuming and

even unfeasible. As a consequence the possibility of identifying empirical input/output models from plant data is particularly attractive to the industrial practitioner. Nonlinear input/output models may be obtained, for example, using dynamic neural networks,⁹ polynomial autoregressive moving average (ARMA) models, or NARMA (nonlinear ARMA) models. The most critical issue in all these models is the introduction of dynamic elements in such a way that multistep output prediction, as required by MPC, can be carried out with reasonable confidence. Moreover, the learning phase requires hundreds of thousands of patterns, even when few input parameters are considered, and these patterns have to be obtained by means of a detailed model or from an existing apparatus. This poses serious problems when the plant performance is affected by one or more parameters that have not been considered in the training of the model. Similarly, if something in the process is modified, the black-box model has to be trained again.

All these problems can be avoided if a detailed, first-principle-based model is used. Unfortunately, the on-line optimization of a detailed model can be an overwhelming task because of the high number of state variables. A novel approach for selecting the variables to be optimized will be shown in the following and will be used to develop an MPC algorithm for a solvent recovery plant involving a pressure-swing distillation (PSD) unit.

Description of the Proposed Algorithm

The procedure proposed in this paper arises from the ideas of Morari et al.¹⁰ and Skogestad and Postlethwaite¹¹ and allows the selection of one variable (or a small number of variables) that will be optimized in the MPC algorithm. The method is based on steady-state analysis because the economic performance can be assumed to be a function of the steady-state behavior.

The fundamental of the approach is the mathematical definition of the objective of the operation, that is, a scalar cost function J that has to be minimized. The optimizing control problem is formulated as

$$\min_u J(u, d) \quad (5)$$

with the constraints

$$g(u, d) \leq 0 \quad (6)$$

where u represents the N_u independent variables that can be manipulated and d represents the disturbances, that is, the independent variables that cannot be affected by the control system. The solution of this problem (if a feasible solution exists) is $u_{opt}(d)$, where

$$\min_u J(u, d) = J[u_{opt}(d), d] = J_{opt}(d) \quad (7)$$

A "perfect" model is required to achieve truly optimal operation; moreover, all disturbances have to be measured and the optimization problem has to be solved on-line. This is unrealistic in most cases and the question is if it is possible to find a

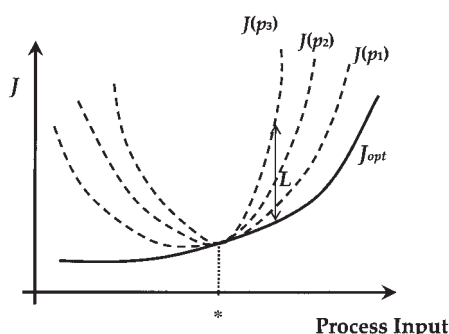


Figure 1. Cost function obtained when all the parameters (continuous line) and when only one parameter (dashed lines) of a process are optimized.

simpler solution that operates satisfactorily, thus with an acceptable loss (L) defined as the difference between the value of the cost function obtained with a specific control strategy and the truly optimal value, that is, $L = J - J_{opt}$.

This idea is illustrated in Figure 1, where it is possible to see that if all the manipulated variables are optimized (in a base case, indicated with “*”) a certain value of the cost function is obtained once the steady state has been reached. If the optimization is repeated for other values of the operating conditions (which can vary because of disturbances and/or process changes) a curve (if we consider only one operating parameter) is obtained, corresponding to the function J_{opt} . This curve represents the best achievable result because it corresponds to the optimization of all the manipulated variables. If only one variable is optimized (with the remaining variables fixed at the optimal values obtained using the base-case parameters) one of the dashed curves can be obtained, depending on the variable considered: all these curves are above that corresponding to J_{opt} because just one variable is optimized, although the value of the loss L is different. More precisely, it should be possible to find one curve for which the loss is minimum. Thus, if only the parameter corresponding to this curve is optimized, it will not be possible to reach J_{opt} , although the loss should be acceptable. The full procedure can be schematized as follows:

Step 1: Degree of Freedom Analysis. Determine the number of degrees of freedom (N_u) available for the control of the process and identify a base set of manipulated variables (u).

Step 2: Cost Function and Constraints Definition. Indicate the scalar cost function J that has to be minimized and the constraints that have to be satisfied.

Step 3: Disturbances Identification. The main disturbances (that is, the independent variables that cannot be affected by the control system) have to be identified; moreover, the range of values that can be assumed by these variables has to be quantified. This range can be determined by means of process analysis, thus making a hypothesis on the values that they can assume. As a general guideline, we suggest considering a variation of the parameters in the range ± 15 – 20% around the base-case values (absence of disturbances).

Step 4: Optimization. Find the values of the N_u manipulated variables that minimize the cost function J , besides fulfilling the operation constraints. Repeat the optimization for some values of the disturbances in the range of values identi-

fied in Step 3. This optimization will result in the curve J_{opt} (see Figure 1), whose point J_{opt}^* has been obtained for the base case.

Step 5: Identify the Variable to be Optimized. Repeat the optimization procedure of Step 4, keeping constant all the manipulated variables at the values resulting in J_{opt}^* , except the variable that is optimized. This will result in various J (and L) curves. The variable that should be optimized is that corresponding to the J curve whose corresponding loss is minimum.

In principle there is no guarantee that the individual J curves do not cross over each other: this can be true when the values of the input parameters are far from those of the base case. As a consequence, if an input variable has a value V that falls in a range where the J curves cross over each other, the above procedure has to be repeated around this point V , which becomes the new base case.

Case Study: The Pressure-Swing Distillation Process

The above-described procedure has been applied to a pressure-swing distillation (PSD) process designed to recover pure ethylacetate from a mixture of water, ethanol, ethylacetate, and other impurities. PSD was proposed in the past to recover a pure component from a mixture if the relative volatility of the components is strongly influenced by the pressure. This operation was proven to be particularly effective when the compounds can form an azeotrope: the change of the pressure may result in a modification of the azeotropic composition and thus it can allow the complete separation of the components.^{12–15}

A sketch of the process is given in Figure 2; the main operating conditions are given in Table 1. The feed is composed mainly of water (52% in mass) and ethylacetate (46%); ethanol, toluene, and isopropanol are the main impurities in the feed. The process is designed to recover at least 95% of the ethylacetate in the feed, with a purity $> 99\%$ of the ethylacetate in the feed, with a purity $> 99\%$. The low-pressure distillation column (C-001) and the high-pressure distillation column (C-002) are integrated energetically through the heat exchanger H-004, which acts at the same time as the condenser of C-002 and as the reboiler of C-001. High-purity ethylacetate is obtained as a bottom product of C-002, whereas the distillate, after cooling to 10°C (in the exchanger H-002), is mixed with

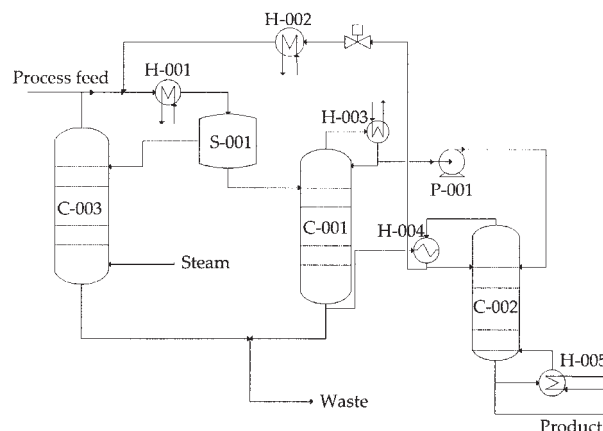


Figure 2. PSD process with the main equipments.

Table 1. Operating Conditions: Base Case

Feeding	
Flow rate	838.2 kg/h
Composition (mass fraction)	
ethanol	0.011
ethylacetate	0.458
water	0.528
toluene	0.002
isopropanol	0.001
Temperature	90°C
Pressure	1 bar
S-001	
Temperature	10°C
Pressure	0.1 bar
C-001	
Feeding stage	3
Number of stages	7
Condenser pressure	0.1 bar
Condenser pressure drop	2.00E-03 bar
Stage pressure drop	4.00E-03 bar
Boil-up ratio	49
C-002	
Feeding stage	2
Number of stages	8
Condenser pressure	5 bar
Column pressure drop	4.00E-02 bar
Reflux ratio	4
Boil-up ratio	6
C-003	
Number of stages	2
Top stage pressure	0.1 bar
Stage pressure drop	4.00E-03 bar
Steam flow rate	30 kg/h
Steam pressure	11.7 bar

the process feed. Because of the ethanol concentration, in the decanter S-001 a heterogeneous liquid–liquid equilibrium is obtained, thus resulting in two liquid product streams: in the first the concentration of ethylacetate is high, and thus it is sent to C-001, whereas the other is sent to the stripper C-003, where the steam recovers the ethylacetate (in the top stream) and removes the ethanol (in the bottom stream).

To give a correct description of the PSD process it is necessary to describe the vapor–liquid equilibrium (VLE) and the liquid–liquid equilibrium (LLE) of the ternary system water–ethanol–ethylacetate: a comparison between results obtained using various thermodynamic models and some experimental data for this system^{16,17} evidenced that the best agreement is obtained when the NRTL model is used to describe the VLE. Similarly, a comparison between the model predictions of the LLE with the experimental data of Griswold et al.¹⁶ proved that the UNIQUAC model is much more adequate; in any case, a better agreement can be obtained if the parameters of the UNIQUAC model are obtained by means of a numerical regression from the experimental data.

The Aspen Plus[®] steady-state simulator was used to simulate the steady state of the process. A recovery of ethylacetate equal to 99.87%, with a mass fraction equal to 99.53% and a heat consumption (in the reboiler of C-002) of about 200 kW are calculated with the operating conditions given in Table 1.

Sensitivity analysis

Before using the above-described procedure to select the variable that has to be optimized on-line, we would point out

the influence of the main manipulated variables on the performance of the process. The variables that can be manipulated are the boil-up ratio of C-001 (BR_{LPC}), the reflux ratio of C-002 (RR_{HPC}), the boil-up ratio of C-002 (BR_{HPC}), the pressure in C-001 (P_{LPC}), and the pressure in C-002 (P_{HPC}). Therefore, the influence of these five variables on the heat duty of the reboiler of the column C-002, which is the cost of the operation that we seek to minimize, is the main focus of this study. Moreover, the influence of the manipulated variables on product purity and recovery (which are the two constraints that have to be fulfilled) has been investigated.

Figures 3–7 show the results of the sensitivity analysis: the parameter in the abscissa is varied, whereas the other four parameters are kept constants at the values used in the base case (see Table 1). When BR_{LPC} is increased (Figure 3) both product recovery and the heat consumption increase, whereas the product purity decreases. Thus, to minimize the cost of the operation besides fulfilling the constraints, the guideline we can follow is to keep BR_{LPC} at the lower value that gives the desired product recovery (and, obviously, the energy integration constraint). When BR_{HPC} is increased (Figure 4) both the heat consumption and the product purity increase, whereas the influence of this parameter on product recovery is more complex; BR_{HPC} should be kept at the lower value in the range where the constraints on product purity and product recovery are satisfied. When RR_{HPC} is increased (Figure 5) the heat duty also increases, whereas the other variables exhibit a maximum. The general guideline in this case is to keep RR_{HPC} at the lower value in the range where the constraints on product purity and recovery are satisfied. Finally, the influence of the pressure in the two columns was considered. Figure 6 exemplifies the influence of P_{LPC} : this value should be kept at the higher value in the range where the constraints on product purity and recovery are satisfied; similar is the guideline that can be derived for the P_{HPC} (Figure 7).

These results give important indications for the optimization: for each operating parameter that can be optimized it is possible to define a range of values where the constraints on product

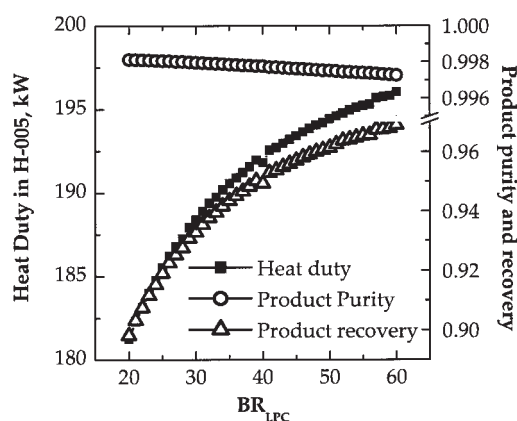


Figure 3. Influence of the boil-up ratio of the low-pressure column on the heat duty of the high-pressure column, on the product purity (given as molar fraction), and on the product recovery ($RR_{HPC} = 4$, $BR_{HPC} = 6$, $P_{LPC} = 0.1$ atm, $P_{HPC} = 5$ atm).

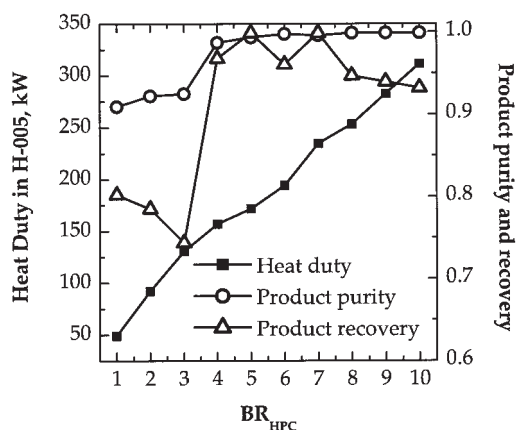


Figure 4. Influence of the boil-up ratio of the high-pressure column on the heat duty of the high-pressure column, on the product purity (given as molar fraction), and on the product recovery ($RR_{HPC} = 4$, $BR_{LPC} = 49$, $P_{LPC} = 0.1$ atm, $P_{HPC} = 5$ atm).

purity and recovery are satisfied. In this region, the minimum of heat consumption is expected to be located at the borders of this region and this can pose serious numerical problems for subsequent optimization.

Steady-state optimization

The optimal operation of the PSD unit corresponds to the minimum of the heat consumption in the reboiler of C-002; the other costs (cooling, pumping, and so on) are considered negligible. As stated in the previous paragraph, there are two constraints that have to be satisfied: a minimum of 95% of the ethylacetate in the feed has to be recovered in the product stream, with a purity $> 99\%$. The SQP algorithm¹⁸ was used to calculate the values of the manipulated variables that minimize the heat consumption. First, the value of all five manipulated

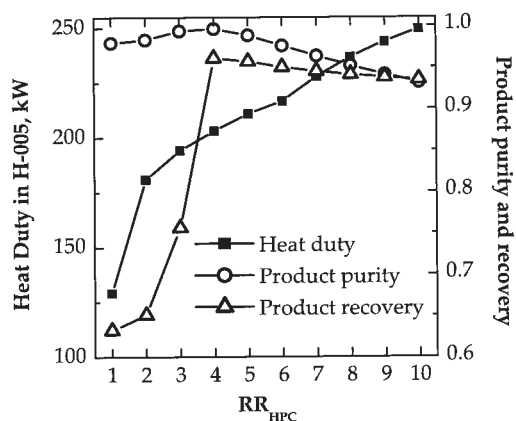


Figure 5. Influence of the reflux ratio of the high-pressure column on the heat duty of the high-pressure column, on the product purity (given as molar fraction), and on the product recovery ($BR_{LPC} = 49$, $RR_{HPC} = 4$, $P_{LPC} = 0.1$ atm, $P_{HPC} = 5$ atm).

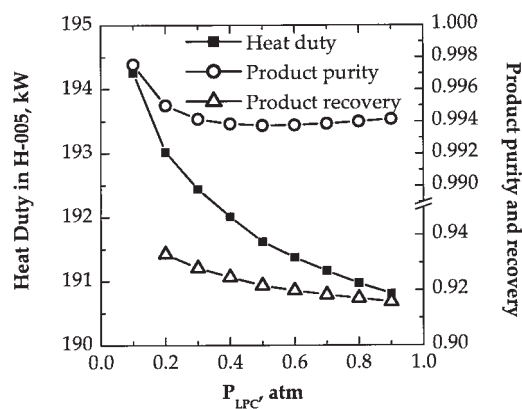


Figure 6. Influence of the pressure in the low-pressure column on the heat duty of the high-pressure column, on the product purity (given as molar fraction), and on the product recovery ($BR_{LPC} = 49$, $RR_{HPC} = 4$, $BR_{HPC} = 6$, $P_{HPC} = 5$ atm).

variables (BR_{LPC} , RR_{HPC} , BR_{HPC} , P_{HPC} , P_{LPC}) has been optimized. If no disturbance affects the operation, it is sufficient to fix the value of these variables to those optimized. Unfortunately, in the process considered, the inlet flow rate can change (the composition is almost constant because it is the result of previous operations); a range $\pm 20\%$ around the base-case value can be considered reasonable. Thus, optimization of the five manipulated variables has been repeated for various values of the process feed flow rate. To find which manipulated variable has the strongest impact on the cost of the operation, the procedure described at the beginning of the paper was applied: each parameter was optimized separately (for various values of the process feed flow rate) with the remaining variables fixed at the optimal values obtained in the base case. The results are shown in Figure 8 (and in Table 2) and evidence that the optimization of the BR_{HPC} can be sufficient to minimize the cost function.

Actually, the pressure in the C-001 can be poorly varied

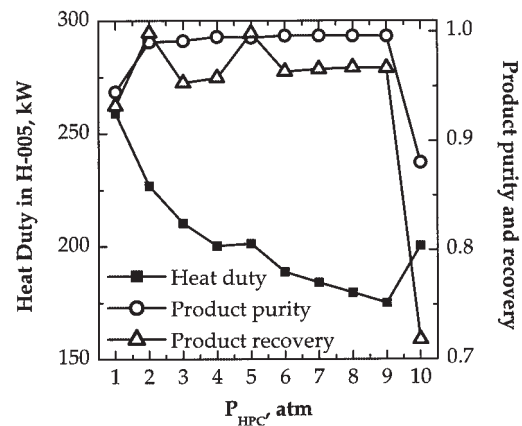


Figure 7. Influence of the pressure in the high-pressure column on the heat duty of the high-pressure column, on the product purity (given as molar fraction), and on the product recovery ($BR_{LPC} = 49$, $RR_{HPC} = 4$, $BR_{HPC} = 6$, $P_{LPC} = 0.1$ atm).

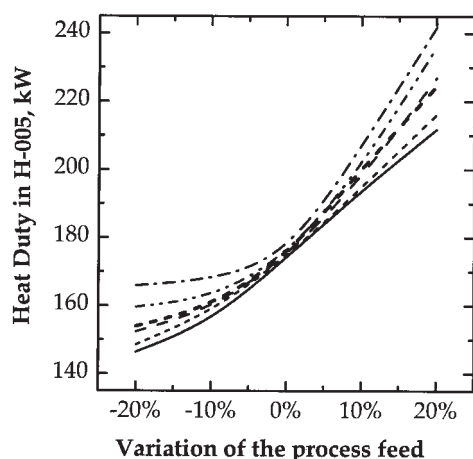


Figure 8. Heat required in the reboiler of the high-pressure column vs. the change in the process feed when BR_{LPC} , RR_{HPC} , BR_{HPC} , P_{LPC} , and P_{HPC} are optimized together (solid line).

The results obtained for the case of optimization of BR_{HPC} (---, $BR_{LPC} = 54.5$, $RR_{HPC} = 4.2$, $P_{LPC} = 0.17$ bar, $P_{HPC} = 7$ bar), for the optimization of RR_{HPC} (- · - · -, $BR_{HPC} = 5.1$, $BR_{LPC} = 54.5$, $P_{LPC} = 0.17$ bar, $P_{HPC} = 7$ bar), for the optimization of the BR_{LPC} (· · · · ·, $RR_{HPC} = 4.2$, $BR_{HPC} = 5.1$, $P_{LPC} = 0.17$ bar, $P_{HPC} = 7$ bar), for the optimization of the P_{LPC} (- · - · -, $BR_{LPC} = 54.5$, $BR_{HPC} = 5.1$, $RR_{HPC} = 4.2$, $P_{HPC} = 7$ bar), and for the optimization of the P_{HPC} (---, $BR_{LPC} = 54.5$, $BR_{HPC} = 5.1$, $RR_{HPC} = 4.2$, $P_{LPC} = 0.17$ bar) are also given.

because it is a consequence of the pressure in S-001, where it is given by a barometric condenser; similarly, the pressure in C-002 should be kept below the project value for reasons of safety. As a consequence the two pressures are not manipulated. The optimization of the other variables (BR_{LPC} , RR_{HPC} , BR_{HPC}) was repeated and the results are given in Table 3 and in Figure 9. The conclusion that can be derived from these results is the same: the optimization of the BR_{HPC} can be sufficient to minimize the cost function.

MPC of the PSD unit

A simplified model was used to carry out optimization in the MPC algorithm (see Appendix A for details). For the algebraic

part the nonlinear equations solver HYBRID1 from the FORTRAN package MINPACK¹⁹ was used, whereas the routine LSODE from ODEPACK library²⁰ was adopted to solve the differential equations. Aspen Plus[®] Dynamic Simulator, which implements a detailed model, was used to validate the simplified model. Extensive investigations were carried out for the validation of the simplified model, in a wide range of operating conditions. Figures 10 and 11 show a few examples where the predictions of the simplified model and those of the detailed model are compared. Figure 10 compares the predictions of the two simulators for the flow rate of ethylacetate in the distillate flow of the low-pressure column and for the heat duty required by the reboiler when the inlet flow rate is decreased by 10% (all the other parameters are set equal to the base-case values). Similarly Figure 11 compares the predictions of the two simulators for the flow rate of ethylacetate in the distillate flow of the high-pressure column and for the heat duty required by the reboiler when the boil-up ratio is decreased by 10%. From these figures, which are just a selection of a large number of comparisons, it is apparent that the proposed simplified model is able to properly describe the dynamic response of the various equipments of the PSD process, both in terms of time constants and of steady-state values.

A standard Newton algorithm was used for the calculation of the optimal sequence of values of the boil-up ratio required to minimize the cost of the operation besides fulfilling the requirements on product purity and recovery. Results are given in Figures 12–14, where the cost function, identified by the heat duty required by the reboiler of the high-pressure column and the values of the manipulated variable are given for various values of the prediction horizon and of the control horizon, which can be considered the most important parameters of the algorithm. The results obtained when the control system is not active are also given to highlight the effectiveness of the MPC algorithm in reducing the cost of the operation in addition to fulfilling the operation constraints on product purity and recovery.

Figures 12 and 13 show the results obtained when the inlet flow rate is decreased (–20% with respect to the base-case value), indicating the influence of both the prediction and the control horizons. The prediction horizon is the number of future intervals when the algorithm evaluates the function that

Table 2. Values of BR_{LPC} , RR_{HPC} , BR_{HPC} , P_{LPC} , and P_{HPC} Obtained When All These Variables Are Optimized Together with Respect to the Change in the Process Feed (Case A)*

Variation of the Process Feed	BR_{LPC}	BR_{HPC}	RR_{HPC} Case A	P_{LPC} , bar	P_{HPC} , bar
–20%	56.2	3.1	5.8	0.24	7.00
–10%	55.4	5.2	4.4	0.18	7.00
0%	54.5	5.1	4.2	0.17	7.00
+10%	50.6	5.8	3.7	0.49	7.00
+20%	44.4	4.6	3.3	0.06	3.02
	Case B	Case C	Case D	Case E	Case F
–20%	43.7	5.3	4.3	0.06	7.0
–10%	44.6	5.2	3.3	0.08	7.0
0%	54.5	5.1	4.2	0.17	7.0
+10%	45.0	5.0	3.8	0.11	7.0
+20%	47.2	4.8	3.5	0.11	7.0

*The result of the optimization is also shown when only one process variable is optimized, that is, BR_{HPC} (case B, $BR_{LPC} = 42.3$, $RR_{HPC} = 4.3$), RR_{HPC} (case C, $BR_{HPC} = 5.1$, $BR_{LPC} = 42.3$), and BR_{LPC} (case D, $RR_{HPC} = 4.3$, $BR_{HPC} = 5.1$).

Table 3. Values of BR_{LPC} , RR_{HPC} , and BR_{HPC} Obtained When All These Variables Are Optimized Together with Respect to the Change in the Process Feed (Case A)*

Variation of the Process Feed	Case A			Case B	Case C	Case D
	BR_{LPC}	BR_{HPC}	RR_{HPC}	BR_{HPC}	RR_{HPC}	BR_{LPC}
-20%	43.3	5.9	4.0	5.4	4.1	44.1
-10%	43.3	5.5	3.9	5.3	3.2	43.9
0%	42.4	5.1	4.3	5.1	4.3	42.4
+10%	41.4	5.0	4.1	4.9	3.8	44.0
+20%	41.2	4.2	3.9	4.7	3.5	46.5

*The result of the optimization is also shown when only one process variable is optimized, that is, BR_{HPC} (case B, $BR_{LPC} = 42.3$, $RR_{HPC} = 4.3$), RR_{HPC} (case C, $BR_{HPC} = 5.1$, $BR_{LPC} = 42.3$), and BR_{LPC} (case D, $RR_{HPC} = 4.3$, $BR_{HPC} = 5.1$).

has to be optimized; for a constant value of the control horizon, the higher the value of NHP, the higher should be the possibility for the control system to predict the future behavior of the process, thus allowing for lower changes in the manipulated variables. The main drawback of using high values of the prediction horizon is that the same values of the disturbance are considered, thus forcing the control system to work on a problem that may differ substantially from the reality—this is clearly indicated in Figure 12, which shows that a value of $NHP = 3$ is sufficient to obtain good results.

The control horizon is the number of future intervals when the value of the manipulated variables is evaluated; for a constant value of the prediction horizon, the higher the value of NHC, the higher the number of degrees of freedom of the controller, which thus becomes much more aggressive. When the value of NHC is lower than the prediction horizon, a constant value of the manipulated variables is used for the time interval between NHP and NHC, thus limiting the possibility of the control system of proposing a more articulated time profile of the manipulated variable. The main drawback of using high values of the control horizon (and thus of the prediction horizon) is that the same values of the disturbance are considered, thus forcing the control system to work on a problem that may

differ substantially from reality. In our system, the influence of the control horizon on the performance of the algorithm seems to be quite poor and a value of $NHC = 2$ can be considered the optimal choice. The same conclusions can be drawn if the process feed flow rate is increased. Figure 14 shows, as an example, the results obtained when the inlet flow rate is increased by 20% and different values of the NHP are used. Analogous results are obtained for various values of the NHC and thus are not shown.

Conclusions

The problem of developing MPC algorithms for complex plants using first-principle-based models has been addressed in

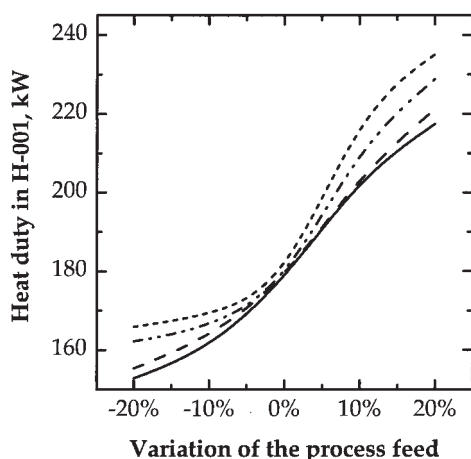


Figure 9. Heat required in the reboiler of the high-pressure column vs. the change in the process feed when BR_{LPC} , RR_{HPC} , and BR_{HPC} are optimized together (solid line).

The results obtained for the case of optimization of BR_{HPC} (---, $BR_{LPC} = 42.4$, $RR_{HPC} = 4.3$), for the optimization of RR_{HPC} (- · - · -, $BR_{HPC} = 5.1$, $BR_{LPC} = 42.4$), and for the optimization of the BR_{LPC} (- - -, $RR_{HPC} = 4.3$, $BR_{HPC} = 5.1$) are also given.

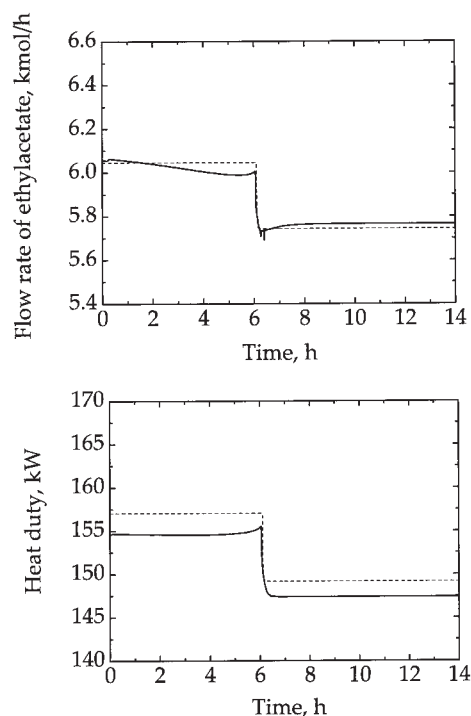


Figure 10. Comparison between the flow rate of ethylacetate in the distillate flow of the low-pressure column (top graph) and the heat duty required by the reboiler of the low-pressure column as predicted by Aspen Plus® Dynamic Simulator (solid line) and by the simplified model (dashed line) when the inlet flow rate decreases by 10% (at $t = 6$ h).

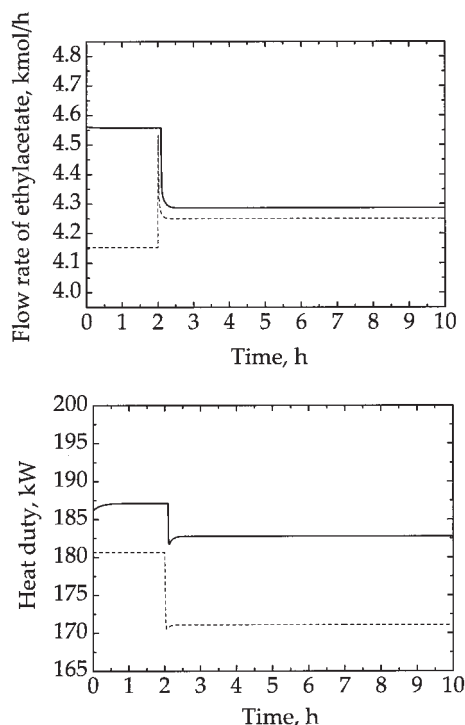


Figure 11. Comparison between the flow rate of ethylacetate in the distillate flow of the high-pressure column (top graph) and the heat duty required by the reboiler of the high-pressure column as predicted by Aspen Plus® Dynamic Simulator (solid line) and by the simplified model (dashed line) when the boil up ratio decreases by 10% (at $t = 2$ h).

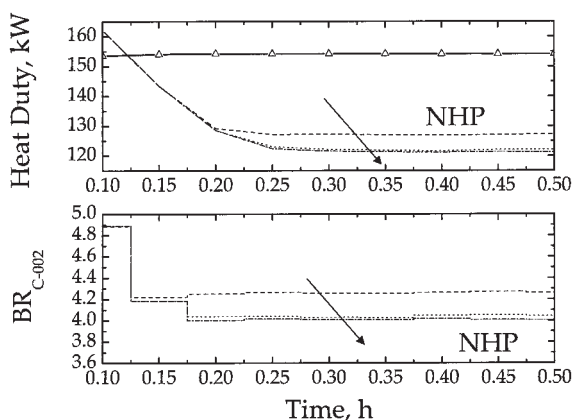


Figure 12. Comparison between the heat required in the reboiler of the high-pressure column (top graph) when the inlet flow rate is decreased (–20%) and the control system is not active (line with symbols) and when the MPC algorithm is active (---, NHP = 2, – · – · – ·, NHP = 3, · · ·, NHP = 4; NHC = 2).

The bottom graphs shows the values of the manipulated variable as calculated by the MPC algorithm for the various values of the parameters.

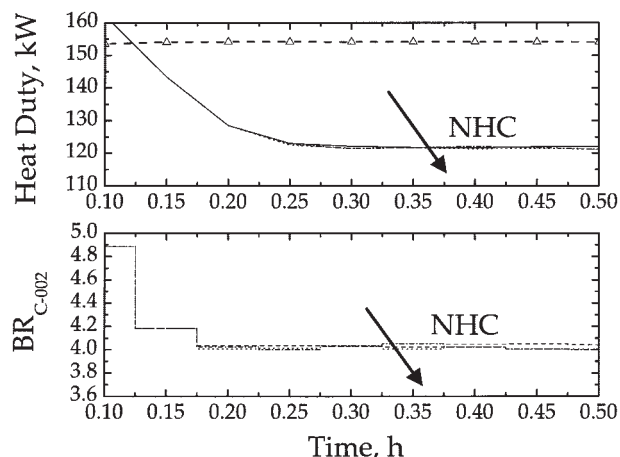


Figure 13. Comparison between the heat required in the reboiler of the high-pressure column (top graph) when the inlet flow rate is decreased (–20%) and the control system is not active (line with symbols) and when the MPC algorithm is active (---, NHC = 2, – · – · – ·, NHC = 3, · · ·, NHC = 4; NHP = 4).

The bottom graphs shows the values of the manipulated variable as calculated by the MPC algorithm for the various values of the parameters.

this article. A new approach based on steady-state optimization was used to reduce the number of variables to be optimized on-line: only those variables whose impact on the objective of the operation is strongest are optimized, thus reducing the computational effort of the control system. A pressure-swing distillation plant was used as case study for the proposed procedure, evidencing the feasibility of using a detailed model

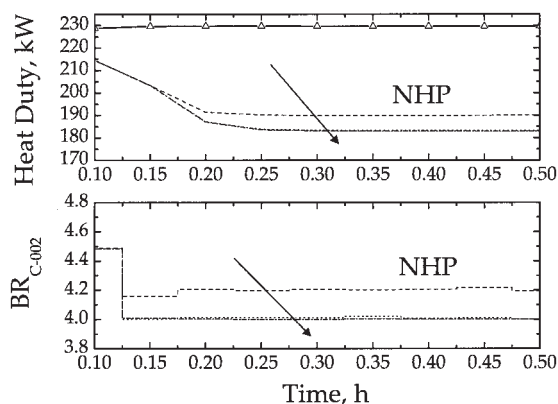


Figure 14. Comparison between the heat required in the reboiler of the high-pressure column (top graph) when the inlet flow rate is increased (+20%) and the control system is not active (line with symbols) and then the MPC algorithm is active (---, NHP = 2, – · – · – ·, NHP = 3, · · ·, NHP = 4; NHC = 2).

The bottom graphs shows the values of the manipulated variable as calculated by the MPC algorithm for the various values of the parameters.

in the MPC algorithm when the proposed procedure is followed.

Acknowledgments

D. Fissore is grateful for a Regione Piemonte Fellowship (SINAPSI, Project No. SPSL-069/14/10/03/12.20). Thanks are due to Prof. Davide Manca (Politecnico di Milano, Italy) for invaluable help in development of the MPC code.

Notation

C = number of components
 d = process disturbance
 E_n = internal energy for liquid holdup on tray n , kJ
 F = feed to the decanter, kmol/h
 $F_{i,n}$ = feed flow rate of component i to tray n , kmol/h
 h_c = control horizon
 h_p = prediction horizon
 H_n^F = molar enthalpy of feed to tray n , kJ/kmol
 H_n^L = molar enthalpy of liquid leaving tray n , kJ/kmol
 H_n^V = molar enthalpy of vapor leaving tray n , kJ/kmol
 J = scalar cost function
 k_i = partition coefficient of species i between the two liquid streams leaving the decanter
 $K_{i,n}$ = liquid–vapor equilibrium coefficient for species i on tray n
 L = loss function
 L_n = liquid flow rate from tray n , kmol/h
 $M_{i,n}$ = liquid holdup of species i in stage n , kmol
 M_n^* = holdup reference value on tray n defined by Eq. A3, kmol
 $n_{a, nb}$ = number of time interval where the input (output) is considered
 P = pressure, bar
 $P_{v,i,n}$ = vapor pressure of component i in stage n , bar
 ΔP_n = pressure drop in stage n , bar
 Q_n = heat duty to tray n , kJ/h
 u = manipulated variable
 U_n = liquid sidestream from tray n , kmol/h
 V_n = vapor flow rate from tray n , kmol/h
 W_n = vapor sidestream from tray n , kmol/h
 $x_{i,n}$ = liquid mole fraction of species i on tray n
 y = process variable
 \hat{y} = prediction of the model for variable y
 $y_{i,n}$ = vapor mole fraction of species i on tray n
 y_{set} = set point value for variable y
 z_i = molar fraction of the i th component in the feed of the decanter

Greek letters

$\gamma_{i,n}$ = activity coefficient of the i th species in stage n
 δ = modeling mismatch with the process
 τ^L = liquid time constant, h
 τ^V = vapor time constant, h
 ω_u = penalty factor for changes between two subsequent control actions
 ω_y = penalty factor for offset of the controlled variable

Subscripts and superscripts

i = species index
 n = tray index
 opt = corresponds to the minimum of the cost function
I, II = indicates the liquid streams leaving the decanter

Abbreviations

BR = boil-up ratio
HPC = high-pressure column
LPC = low-pressure column
MPC = model predictive control
PSD = pressure-swing distillation
RR = reflux ratio

Literature Cited

- Garcia CE, Prett DM, Morari M. Model predictive control: Theory and practice—A survey. *Automatica*. 1989;25:335–348.
- Ricker NL. Model predictive control: State of the art in chemical process control. In Arkun Y, Ray WH, eds. *Proceedings of CPC IV, Fourth International Congress on Chemical Process Control*. Amsterdam, The Netherlands: Elsevier; 1991:271–279.
- Morari M, Lee JH. Model predictive control: The good, the bad, and the ugly, in chemical process control. In Arkun Y, Ray WH, eds. *Proceedings of CPC IV, Fourth International Congress on Chemical Process Control*. Amsterdam, The Netherlands: Elsevier; 1991:419–427.
- Morari M, Lee JH. Model predictive control: Past, present and future. *Comput Chem Eng*. 1999;23:667–682.
- Muske KR, Rawlings JB. Model predictive control with linear models. *AIChE J*. 1993;39:262–287.
- Lee JH. Recent advances in model predictive control and other related areas. In Kantor JC, Garcia CE, Carnahan B, eds. *Proceedings of CPC V, Fifth International Congress on Chemical Process Control, AIChE Symposium Series*, Tahoe City, CA; 1996:201–209.
- Ogunnaike BA, Ray WH. *Process Dynamics, Modelling and Control*. New York, NY: Oxford Univ. Press; 1994.
- Henson MA, Seborg DE. *Nonlinear Process Control*. Englewood Cliffs, NJ: Prentice Hall; 1997.
- Psichogios DC, Ungar LH. Direct and indirect model based control using artificial neural networks. *Ind Eng Chem Res*. 1991;30:2564–2573.
- Morari M, Arkun Y, Stephanopoulos G. Studies in the synthesis of control structures for chemical processes. Part I: Formulation of the problem. Process decomposition and the classification of the control task. Analysis of the optimizing control structures. *AIChE J*. 1980;26:220–232.
- Skogestad S, Postlethwaite I. *Multivariable Feedback Control*. Chichester, UK: Wiley; 1996.
- Knapp JP, Doherty MF. A new pressure-swing distillation process for separating homogeneous azeotropic mixtures. *Ind Eng Chem Res*. 1992;31:346–357.
- Frank TC. Break azeotropes with pressure-sensitive distillation. *Chem Eng Prog*. 1997;93:52–63.
- Horwitz BA. Optimize pressure-sensitive distillation. *Chem Eng Prog*. 1997;93:47–51.
- Hamad A, Dunn RF. Energy optimisation of pressure-swing azeotropic distillation systems. *Ind Eng Chem Res*. 2002;41:6082–6093.
- Griswold J, Chu PL, Winsauer WO. Phase equilibria in ethyl alcohol–ethyl acetate–water system. *Ind Eng Chem*. 1949;41:2352–2358.
- Lee LS, Chen WC, Huang JF. Experiments and correlations of phase equilibria of ethanol–ethyl acetate–water ternary mixtures. *J Chem Eng Jpn*. 1996;29:427–438.
- Boggs PT, Tolle JW. Sequential quadratic programming. *Acta Numer*. 1995;51.
- More JJ, Garbow BS, Hillstom KE. *User Guide for MINPACK*. Argonne, IL: Argonne National Laboratory; 1980.
- Hindmarsh AC. *ODEPACK, A Systematized Collection of ODE Solvers*. Amsterdam, The Netherlands: Scientific Computing; 1983.

Appendix A: Simplified Model of the PSD Plant

Each *distillation column* has been considered as a sequence of equilibrium stages; each of them can have a liquid and a vapor sidestream (indicated with U and W , respectively), one feed (F), and one thermal duty. The column has N vapor–liquid theoretical trays numbered from the reboiler (stage 1) up to the top tray of the column (stage N), plus the condenser–decanter system. Consider a stage n : the streams exiting from this stage are identified with the subscript n , whereas the streams identified with $n - 1$ are those arriving from the preceding stage and those identified with $n + 1$ are arriving from the following stage in the sequence. In formulating the model capacitance, terms arising from the downcomers are neglected, as well as the vapor holdup over the plate; moreover, the liquid and vapor

phases are considered to be well mixed and the liquid and vapor streams leaving each stage are considered to be in phase equilibrium. If there are C components in the column, then the following $(C + 5)$ equations can be written for each stage

C Material Balances

$$\frac{dM_{i,n}}{dt} = L_{n+1}x_{i,n+1} - (L_n + U_n)x_{i,n} - (V_n + W_n)y_{i,n} + V_{n-1}y_{i,n-1} + F_{i,n} \quad i = 1, \dots, C \quad (\text{A1})$$

One Energy Balance

$$\frac{dE_n}{dt} = L_{n+1}H_{n+1}^L - (L_n + U_n)H_n^L - (V_n + W_n)H_n^V + V_{n-1}H_{n-1}^V + F_nH_n^F + Q_n \quad (\text{A2})$$

Two Fluid Dynamic Relationships

$$\sum_{i=1}^C M_{i,n} = M_n^* - \tau^V(V_n + W_n) + \tau^L(L_n + U_n) \quad (\text{A3})$$

$$P_n = P_{n+1} + \Delta P_{n+1}(L_n, V_n, U_n, W_n, \text{geometry}) \quad (\text{A4})$$

One Vapor-liquid Equilibrium Equation

$$\sum_{i=1}^C K_{i,n}x_{i,n} = 1 \quad (\text{A5})$$

where $K_{i,n} = P_{V,i,n}\gamma_{i,n}/P_n$ and $P_{V,i,n}$ is the vapor pressure of the component i on stage n and γ_i is its activity coefficient.

One Definition of the Total Energy per Plate

$$E_n = H_n^L \sum_{i=1}^C M_{i,n} \quad (\text{A6})$$

The model is thus constituted by an algebraic-differential system of equations; at each time step we can obtain the following state variable for every stage: temperature (T_n), pressure (P_n), total energy (E_n), total molar holdup of each component ($M_{i,n}$), and the liquid (L_n) and vapor (V_n) flow rates leaving the stage.

Equations A3 and A4 reflect the level of fluid dynamic simplification used in the model. The constants M_n^* , τ^L , and τ^V depend on the particular type of plate and on the geometric characteristics of the column; moreover, the definition of the pressure profiles in the column needs the evaluation of pressure drops across each tray. Values of these constants were calculated by means of numerical regression from the results obtained with Aspen Plus[®] steady-state simulator.

The *stripper* was modeled as a sequence of two equilibrium stages working in isothermal conditions; thus the same system of equations previously described can be used.

The *decanter* was modeled as an equilibrium stage with two liquid streams in equilibrium leaving the drum (indicated with I and II). The presence of a vapor phase in equilibrium with the two liquids was neglected. Temperature and pressure are assumed to be known and constant.

Manuscript received July 18, 2005; revision received Apr. 3, 2006; and final revision received Jun. 28, 2006.